Trying to bring the magnetopause to a standstill

J. De Keyser, F. Darrouzet, and M. Roth
Belgian Institute for Space Aeronomy, Brussels, Belgium

Received 27 February 2002; revised 19 April 2002; accepted 19 April 2002; published 28 May 2002.

[1] Satellite observations of the magnetospheric boundary (magnetopause and boundary layer) show it to be a very dynamic place, in part due to boundary motion. We present a straightforward technique for identifying boundary motion and for recovering magnetopause and boundary layer structure in a reference frame that comoves with the boundary, that is, a frame in which it is at a standstill. *INDEX TERMS:* 2724 Magnetospheric Physics: Magnetopause, cusp, and boundary layers; 2784 Magnetospheric Physics: Solar wind/magnetosphere interactions; 7811 Space Plasma Physics: Discontinuities

1. Introduction

[2] The boundary of the Earth's magnetosphere consists of the magnetopause (MP) and the boundary layer (BL). Satellite observations of the MP/BL are difficult to interpret because of the time variability of plasma and field observations near the boundary. Understanding this variability is essential, since most processes of mass and energy transfer across the boundary are dynamic. The signatures of such processes are obscured by boundary motion: The boundary frantically moves in- and outward in response to solar wind pressure variations [*Song et al.*, 1988; *Sibeck et al.*, 1991] or as a consequence of surface instabilities [*Sckopke et al.*, 1981; *Kivelson and Chen*, 1995]. This radial motion can be quite fast, up to 80 km s^{-1} or more [*Berchem and Russell*, 1982; *Bauer et al.*, 2000].

[3] In this paper we develop a straightforward method to deal with boundary motion. We simultaneously determine (1) MP/BL position as a function of time and (2) the spatial structure of the plasma and field transitions in a frame fixed to the boundary. In section 2 we introduce the underlying model. Section 3 focuses on the technique used to recover boundary position and the transition profiles. In section 4 we present an example. We conclude with a brief discussion.

2. Model

[4] The MP/BL oscillates in response to changes in solar wind pressure. This oscillatory motion implies nonzero acceleration and thus, in principle, precludes an understanding of the boundary in terms of a moving equilibrium structure. In practice, however, the equilibrium does not strongly change while the boundary is moving. For instance, taking the magnetic field near the MP/BL to be just the dipole field, a MP/BL at a standoff distance of $x_{MP/BL} = 10\ R_E$ moves earthward over $\delta x = -1000$ km for a change in total pressure of only $\delta p_{tot}/p_{tot} \sim -6\delta x/x_{MP/BL}(1 + \beta_{MP/BL}) = 5\%$ (taking $\beta_{MP/BL} \sim 1$ and neglecting its variation). The boundary therefore is never at rest: Solar wind pressure fluctuations of that magnitude are always present. Larger pressure changes do significantly affect boundary structure; the MP/BL then moves over substantially larger distances. Cases where boundary motion was gentle enough so as to lead to an essentially rigid structure moving back and forth have been reported before [*Hubert et al.*, 1998].

[5] We assume that the MP/BL can be modeled as a tangential discontinuity (TD). Given a time sequence of magnetic field observations $\mathbf{B}_i = \mathbf{B}(t_i)$, the instantaneous orientation of the TD surface is determined by the local normal $\mathbf{n}_i = \mathbf{B}_i \times (\mathbf{B}_{i+1} - \mathbf{B}_{i-1})/\|\mathbf{B}_i \times (\mathbf{B}_{i+1} - \mathbf{B}_{i-1})\|$. In the boundary crossings we have looked at, minimum variance analysis of $\mathbf{n}$ reveals that there is one particular direction in which $\mathbf{n}$ almost doesn't change (often the geomagnetic field direction), which we will label z, while $\mathbf{n}$ remains essentially in the plane perpendicular to it (the xy plane): The shape of the TD can be described by a curve in the xy plane that may change with time. We limit the discussion to the situation where $\mathbf{n}$ is essentially constant (after filtering out high frequency noise). The boundary can then be modeled as a planar TD (a wavy surface in the long wavelength limit) in which the field and plasma parameters only depend on the x coordinate, perpendicular to the TD. We now introduce a reference frame XYZ, oriented just like xyz, but fixed to the MP/BL, which we consider to move as a rigid structure. Suppose the MP/BL position $\hat{x}$ as a function of time is known. Measurements made by a spacecraft at x_{sc} in the xyz frame then correspond to a position $X_{sc}(t) = x_{sc}(t) - \hat{x}(t)$ in the comoving XYZ frame. We can construct an estimate for $\hat{x}$: In a rigidly moving structure the locally measured plasma velocity v_{obsx} is the boundary velocity. A proxy for MP/BL position then is

$$\hat{x}_{obs}(t) = \int_{t_0}^{t} v_{obsx}(t')dt' \ + \ x_{sc}(t_0).$$

To be precise, $\hat{x}_{obs}$ is the position of the magnetic surface (a plane defined by $X = ct$) on which the spacecraft was located at a reference time t_0. As MP/BL motion can be highly oscillatory, v_{obsx} must be known with adequate time resolution to allow accurate tracking of $\hat{x}_{obs}(t)$. As t and t_0 are farther apart the uncertainty on the position due to the observational errors δv_{obsx} grows so that the relative accuracy on $\hat{x}_{obs}$ decreases. For instance, a small systematic error of only 1 km s^{-1} adds up to a position error of 1/2 R_E after integrating over an hour. The idea of using the locally measured plasma velocity to track MP/BL position is not new [*Paschmann et al.*, 1990; *Phan and Paschmann*, 1996].

[6] We introduce the model MP/BL position profile $\hat{x}_{model}(t)$, which we represent by a piecewise linear spline whose nodes are the plasma velocity sampling times t_i and which is defined by its values $\hat{x}_{model\,i}$ at the nodes. The model boundary velocity is denoted by $\hat{v}_{model} = d\hat{x}_{model}/dt$. We adopt a magnetostatic model of the MP/BL that incorporates a smooth transition between the magnetosheath and magnetospheric plasmas and a rotation of the tangential magnetic field. We define transition functions with halfwidth d centered at X_0,

$$\phi_{\pm}(X; X_0, d) \ = \ \frac{1}{2}\left(1 \ \pm \ \tanh\frac{X - X_0}{d}\right),$$

where $\phi_- + \phi_+ = 1$. Let $\phi_{p\pm}(X) = \phi_{\pm}(X; X_{0p}, d_p)$ and $\phi_{b\pm}(X) = \phi_{\pm}(X; X_{0b}, d_b)$ represent the transitions in plasma density and magnetic

0094-8276/02/2002GL015001

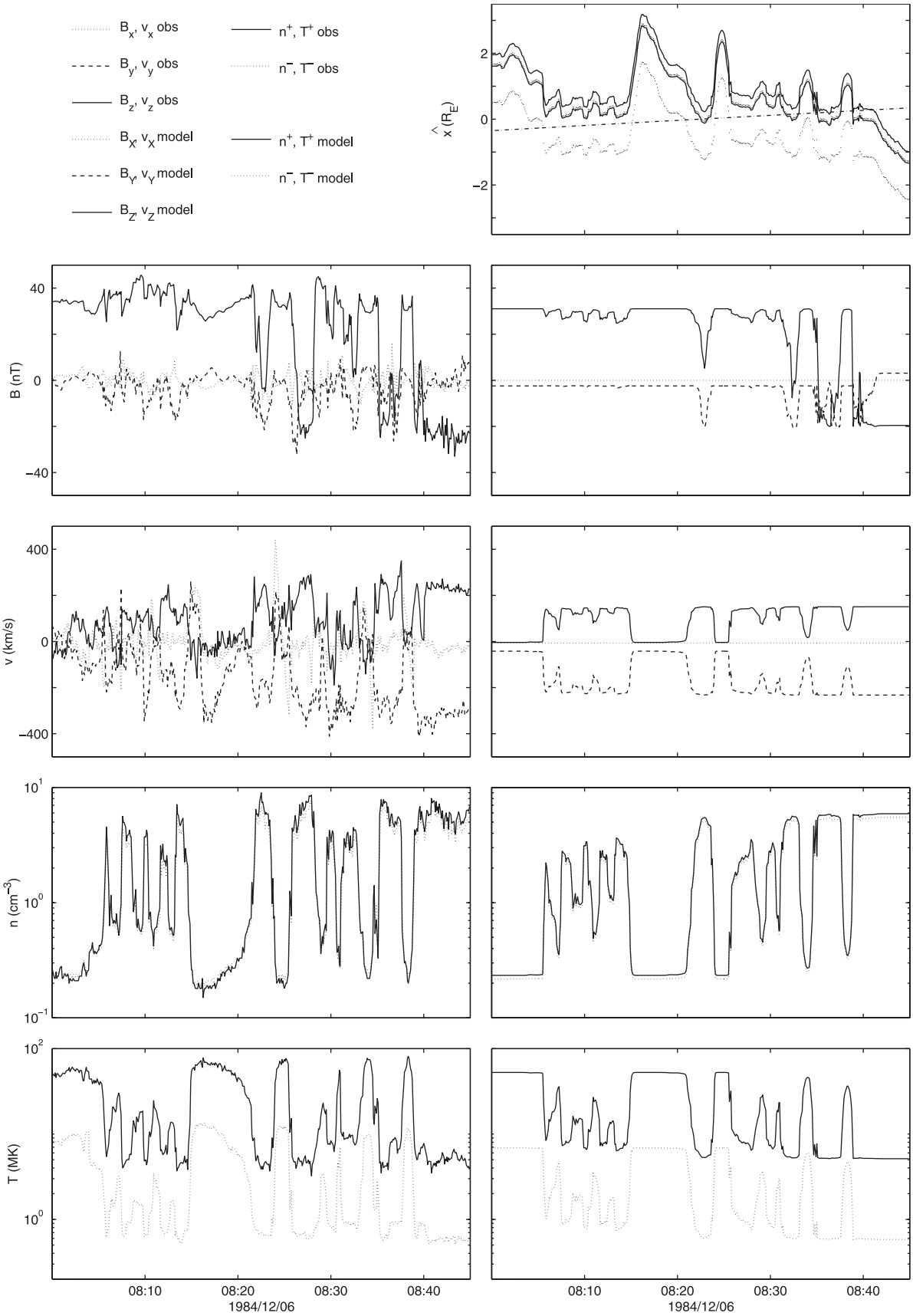

Figure 1. Observed magnetic field, velocity, density, and temperature (left) recorded by AMPTE/IRM during part of its dawn flank magnetospheric boundary crossing on December 6, 1984, as well as their reconstructed values (right). The reconstructed boundary position is shown in the top right plot.

field orientation. Density, ion and electron temperature, and velocity are given by

$$n_{\text{model}} = n_L\phi_{p-} + n_R\phi_{p+},$$
$$T^{\pm}_{\text{model}} = \left[T^{\pm}_L n_L\phi_{p-} + T^{\pm}_R n_R\phi_{p+}\right]/n_{\text{model}},$$
$$v_{\text{model}\,X} = v_{\text{model}\,x} - \hat{v}_{\text{model}\,x} = 0,$$
$$v_{\text{model}\,Y} = v_{\text{model}\,y} = \left[v_{yL} n_L\phi_{p-} + v_{yR} n_R\phi_{p+}\right]/n_{\text{model}},$$
$$v_{\text{model}\,Z} = v_{\text{model}\,z} = \left[v_{zL} n_L\phi_{p-} + v_{zR} n_R\phi_{p+}\right]/n_{\text{model}},$$

where n_L, n_R, $T^{\pm}_L$, $T^{\pm}_R$, v_{yL}, v_{yR}, v_{zL}, v_{zR} are constant model parameters. The densities that would be detected by ion and electron instruments are

$$n^{\pm}_{\text{model}} = n_{\text{model}}/\alpha^{\pm};$$

the constants $\alpha^{\pm}$ account for density calibration differences. The magnetic field is modeled by

$$\theta_{\text{model}} = \theta_L\phi_{b-} + \theta_R\phi_{b+},$$
$$B^2_{\text{model}} = 2\mu_0\left[p_{\text{tot}} - n_{\text{model}}k_B\left(T^{+}_{\text{model}} + T^{-}_{\text{model}}\right)\right],$$
$$B_{\text{model}\,X} = B_{\text{model}\,x} = 0,$$
$$B_{\text{model}\,Y} = B_{\text{model}\,y} = B_{\text{model}}\cos\theta_{\text{model}}$$
$$B_{\text{model}\,Z} = B_{\text{model}\,z} = B_{\text{model}}\sin\theta_{\text{model}},$$

with k_B Boltzmann's constant and μ_0 the vacuum magnetic permeability, and where p_{tot}, θ_L, and θ_R are model parameters. This model reflects typical MP/BL structure [*Phan and Paschmann*, 1996].

3. Method

[7] Consider the observables $\mathbf{q} = [\hat{x}, B_x, B_y, B_z, v_x, v_y, v_z, \log n^{\pm}, \log T^{\pm}]$. For these observables, we have model values $\mathbf{q}_{\text{model}}$ and observations $\mathbf{q}_{\text{obs}}$ with error bars $\delta\mathbf{q}_{\text{obs}}$. By matching both, that is, by minimizing

$$G^2 = \sum_q w_q^2 \sum_i \left(\frac{q_{\text{obs}}(x_{\text{sc}}(t_i)) - q_{\text{model}}(X_{\text{sc}}(t_i))}{\delta q_{\text{obs}}(x_{\text{sc}}(t_i))}\right)^2 > 0,$$

we determine the model parameters and the changing MP/BL position. This is a least-squares optimization problem. The outer sum is over each observable q. The quantities $w_q^2 > 0$ are given weight factors. The inner sum runs over all observation points. We interpolate all observations onto the plasma velocity time sampling t_i since these measurements inherently limit the precision of $X_{\text{sc}}(t_i)$. Each inner sum measures the deviation between data and model, relative to the uncertainty on the data.

[8] Minimizing G^2 to determine $\hat{x}_{\text{model}i}$ and the model parameters p_k is a nonlinear problem. The requirements $\partial G^2/\partial\hat{x}_{\text{model}i} = 0$ are nonlinear, but each requirement involves only terms in the expression for G^2 for time t_i, so that they all are mutually independent (but they do depend on the model parameters p_k). The requirements $\partial G^2/\partial p_k = 0$ result in a linear system for only a subset of the parameters, namely for v_{yL}, v_{yR}, v_{zL}, and v_{zR}:

$$\begin{bmatrix} \sum_i \mu_{iL}^2 & \sum_i \mu_{iL}\mu_{iL} \\ \sum_i \mu_{iL}\mu_{iR} & \sum_i \mu_{iR}^2 \end{bmatrix} \begin{bmatrix} v_{\{y,z\}R} \\ v_{\{y,z\}L} \end{bmatrix} = \begin{bmatrix} \sum_i \mu_{iL} v_{\{y,z\}i} \\ \sum_i \mu_{iR} v_{\{y,z\}i} \end{bmatrix},$$

where $\mu_{i\{L,R\}} = n_{\{L,R\}}\phi_{p\{-,+\}}(X_i)/n(X_i)\,\partial v_i$. The equations $\partial G^2/\partial\alpha^{\pm}$ are nonlinear but explicitly solvable:

$$\log\alpha^{\pm} = \frac{\sum_i \left(\log n(X_i) - \log n_i^{\pm}\right)/\left(\delta\log n_i^{\pm}\right)^2}{\sum_i 1/\left(\delta\log n_i^{\pm}\right)^2}.$$

We exploit the structure of the problem to facilitate the optimization. We use a simple but robust scheme to explore the subspace of variables X_{0p}, d_p, n_L, n_R, $T^{\pm}_L$, $T^{\pm}_R$, p_{tot}, X_{0b}, d_b, θ_L, and θ_R, as well as all the $\hat{x}_{\text{model}i}$, while the above equations are used to obtain the corresponding optimal values for v_{yL}, v_{yR}, v_{zL}, v_{zR}, and $\alpha^{\pm}$. The optimization is stopped when the parameters are known up to a prescribed accuracy; we typically require 6 significant digits. Once we have established the parameter values, we compare the observed time profiles $q_{\text{obs}}(x_{\text{sc}}(t))$ with the reconstructed ones $q_{\text{model}}(X_{\text{sc}}(t))$ to assess the quality of the fit. We can also compare the observations $[X_{\text{sc}}(t), q_{\text{obs}}(X_{\text{sc}}(t))]$ and the model $[X, q_{\text{model}}(X)]$ in the *XYZ* frame.

4. Results

[9] We illustrate the method for an Active Magnetospheric Particle Tracer Explorer/Ion Release Module (AMPTE/IRM) outbound dawnside MP/BL crossing on December 6, 1984, near 0700 local time. We use 5 second resolution data from the three-dimensional plasma electrostatic analyzer [*Paschmann et al.*, 1985] and from the fluxgate magnetometer [*Lühr et al.*, 1985]. This crossing represents a tough test case, with more than 20 large amplitude density/temperature variations in quick succession in 2 hours time. We have selected the 0800 to 0845 UT subinterval, which contains 10 of these variations. Changes in plasma properties are coincident with partial or full transitions from the geomagnetic to the magnetosheath magnetic field. For this time interval, we compute the minimum variance frame based on $\mathbf{n}$ (x', y', and z are the maximum, intermediate, and minimum variance directions, respectively) and further rotate over 26° in the $x'y'$ plane to obtain the xyz frame, in which x is the average outward normal to the MP/BL (the angle is chosen such that the method works best). The resulting frame is $\mathbf{x} = [0.602, -0.797, 0.050]$, $\mathbf{y} = [0.643, 0.521, 0.561]$, $\mathbf{z} = [-0.471, -0.305, 0.826]$ (in GSE coordinates). We then fit the model to the observations, guided by absolute errors $\delta\hat{x} = 0.05\ R_E$, $\delta B = 1$ nT, and $\delta v = 20$ km s^{-1}, and relative errors $\delta n^{\pm} = 5\%$ and $\delta T^{\pm} = 5\%$. Weight $w_{\hat{x}}^2$ is chosen to be 5, while the other weights are unity. The top right plot in Figure 1 shows the reconstructed position of the MP/BL as a function of time (reference $\hat{x} = 0$ was chosen arbitrarily; the magnetosheath is to the top, the magnetosphere to the bottom). The dot-dashed straight line is the satellite track. Solid lines delineate the field rotation at the MP ($X_{0b} \pm d_b$, $\sim$0.2 R_E thick), while dotted lines indicate the BL ($\sim$1 R_E thick, between $X_{0p} + d_p$ and $X_{0p} - 3d_p$, reflecting the changes in the logarithms of density and temperature), which is found to be located earthward of the MP but adjacent to it, as expected. MP/BL position fluctuates over $\pm$1 R_E, in agreement with earlier observations [*Song et al.*, 1988]. The other plots in Figure 1 show the observations (left column) and their reconstructed version using the model profiles and using the reconstructed MP/BL position (right column). The agreement is quite good but not perfect. There is a difference, for instance, for the partial B_z reversal and the density changes near 0827 UT. This is due to the very rapid normal velocities, in excess of 400 km s^{-1}, recorded near 0824 UT. Together with the limited time resolution, such rapid fluctuations make tracking of MP/BL position inherently difficult. Nevertheless, in this case it is clear that the observed transients are intimitely related to boundary motion. This interpretation of transients is compatible with two-point measurements of MP/BL structure [*Sibeck et al.*, 2000]. We checked that the pressure balance assumption holds up well in this example. We do expect some deviations to come from surface curvature; if the observed quasi-periodic structures are waves (period $\sim$ 100 s), convecting tailward with the magnetosheath velocity (200 km s^{-1}), the wavelengths exceed 3 R_E, so that the long-wavelength approximation is reasonable.

5. Discussion

[10] We have examined to what extent MP/BL observations can be interpreted in terms of a one-dimensional quasi-static equilibrium moving back and forth. We have done so by proposing spatial profiles across the MP/BL for all plasma and field characteristics and by using the local plasma velocity to track

boundary motion, and then solving a nonlinear optimization problem. The model simultaneously matches the magnetic field and plasma observations. An important aspect is that we treat the changing MP/BL position itself as a profile that is guided by observation, but fitted during the optimization. The degree of correspondence between fit and observations depends on the associated weight, which reflects the limited confidence we have in the plasma velocity observations and their ability to track boundary position, especially when the velocities are large and strongly variable.

[11] We have found that MP/BL motion can explain the observed time variability during a number of crossings. In those cases the quality of the result serves as an a posteriori justification of the static one-dimensional model. As a bonus, we obtain reasonable magnetopause current layer and boundary layer thickness estimates [*Phan and Paschmann*, 1996] without the need for multi-satellite observations [*Berchem and Russell*, 1982; *Bauer et al.*, 2000].

[12] The proposed model has several limitations: (1) It imposes a specific and simple form of the transition profiles, while in reality these might be more complicated (non-monotonous, multiple length scales, . . .). The model can be readily extended to allow a larger variety of transition profiles, at the expense of increasing the number of parameters. (2) Problems arise when the MP/BL motion is not well reconstructed, for instance, when the velocity data time resolution is insufficient; a sampling rate of 0.1 Hz seems to be the minimum. (3) When there are short-wavelength surface waves on the boundary, a one-dimensional model is no longer appropriate; in such cases it is not trivial to relate the local plasma velocity to the motion of the boundary. (4) Rapid large-amplitude boundary motion may affect boundary structure, so that the use of a quasi-static equilibrium model is not justified. For instance, the model discussed here assumes boundary layer thickness to remain constant, which may not be true. (5) An underlying hypothesis is that the boundary position can be described by a single-valued function $\hat{x}(t)$. This is not true in the final stages of the nonlinear steepening of large-amplitude surface waves [*Otto and Fairfield*, 2000] or when isolated magnetosheath plasma entities exist in the magnetosphere [*Lemaire and Roth*, 1991].

[13] Deviations from the static one-dimensional model indicate whether there are interesting physical phenomena going on. In such cases, it is especially rewarding to analyze multiple satellite observations. The techniques described in this paper can be generalized by including data from all the satellites in the optimization process. Another possibility is to determine position and structure of the MP/BL using data from one satellite, and to predict what the other satellites would see. Initial tests with Cluster data seem promising; we hope to report on this work in the near future.

[14] **Acknowledgments.** The authors thank D. Sibeck and the JHU/APL data center for access to the AMPTE/IRM data. G. Paschmann (Max-Plank-Institut für Extraterrestrische Physik, Garching, Germany) and H. Lühr (Technische Universität Braunschweig, Germany, now at the Geoforschungszentrum Potsdam, Germany) were the PIs for the AMPTE/IRM plasma and magnetic field instruments. This work was supported by the Belgian Federal Office for Scientific, Technical and Cultural Affairs through ESA (PRODEX/Cluster and PRODEX/Solar Drivers of Space Weather).

References

Bauer, T. M., M. W. Dunlop, B. U. Ö. Sonnerup, N. Sckopke, A. N. Fazakerley, and A. V. Khrabrov, Dual spacecraft determinations of magnetopause motion, *Geophys. Res. Lett.*, *27*, 1835–1838, 2000.

Berchem, J., and C. T. Russell, The thickness of the magnetopause current layer: ISEE 1 and 2 observations, *J. Geophys. Res.*, *87*, 2108–2114, 1982.

Hubert, D., C. C. Harvey, M. Roth, and J. De Keyser, Electron density at the subsolar magnetopause for high magnetic shear: ISEE 1 and 2 observations, *J. Geophys. Res.*, *103*, 6685–6692, 1998.

Kivelson, M. G. and S.-H. Chen, The magnetopause: Surface waves and instabilities and their possible dynamical consequences, in *Physics of the Magnetopause, Geophys. Monogr. Ser.*, vol. 90, edited by P. Song, B. U. Ö. Sonnerup, and M. F. Thomsen, pp. 257–268, AGU, Washington, D.C., 1995.

Lemaire, J., and M. Roth, Non-steady-state solar wind-magnetosphere interaction, *Space Sci. Rev.*, *57*, 59–108, 1991.

Lühr, H., N. Klöcker, W. Oelschlägel, B. Häusler, and M. Acuna, The IRM fluxgate magnetometer, *IEEE Trans. Geosci. Remote Sens.*, *23*, 259–261, 1985.

Otto, A., and D. H. Fairfield, The Kelvin-Helmholtz instability at the magnetotail boundary: MHD simulation and comparison with Geotail observations, *J. Geophys. Res.*, *105*, 21,175–21,190, 2000.

Paschmann, G., H. Loidl, P. Obermayer, M. Ertl, R. Laborenz, N. Sckopke, W. Baumjohann, C. W. Carlson, and D. W. Curtis, The plasma instrument for AMPTE/IRM, *IEEE Trans. Geosci. Remote Sens.*, *23*, 262–266, 1985.

Paschmann, G., B. Sonnerup, I. Papamastorakis, W. Baumjohann, N. Sckopke, and H. Lühr, The magnetopause and boundary layer for small magnetic shear: Convection electric fields and reconnection, *Geophys. Res. Lett.*, *17*, 1829–1832, 1990.

Phan, T. D., and G. Paschmann, Low-latitude magnetopause and boundary layer for high magnetic shear, 1, Structure and motion, *J. Geophys. Res.*, *101*, 7801–7815, 1996.

Sckopke, N., G. Paschmann, G. Haerendel, B. U. Ö. Sonnerup, S. J. Bame, T. G. Forbes, E. W. Hones Jr., and C. T. Russell, Structure of the low-latitude boundary layer, *J. Geophys. Res.*, *86*, 2099–2110, 1981.

Sibeck, D. G., R. E. Lopez, and E. C. Roelof, Solar wind control of the magnetopause shape, location, and motion, *J. Geophys. Res.*, *96*, 5489–5495, 1991.

Sibeck, D. G., L. Prech, J. Safrankova, and Z. Nemecek, Two-point measurements of the magnetopause: Interball observations, *J. Geophys. Res.*, *105*, 237–244, 2000.

Song, P., R. C. Elphic, and C. T. Russell, ISEE 1 and 2 observations of the oscillating magnetopause, *Geophys. Res. Lett.*, *15*, 744–747, 1988.

J. De Keyser, F. Darrouzet, and M. Roth, Belgian Institute for Space Aeronomy, Ringlaan 3, B-1180 Brussels, Belgium. (Johan.DeKeyser@bira-iasb.oma.be; Fabien.Darrouzet@bira-iasb.oma.be; Michel.Roth@bira-iasb.oma.be)